Inorg. Chem. **2008**, *47*, 5580−5590

Synthesis and Characterization of a Family of Penta- and Tetra-Manganese(III) Complexes Derived from an Assembly System Containing *tert*-Butylphosphonic Acid

Mei Wang,[†,‡] Cheng-Bing Ma,[†] Da-Qiang Yuan,[†] Hui-Sheng Wang,[†] Chang-Neng Chen,*[,†] and Qiu-Tian Liu[†]

State Key Laboratory of Structural Chemistry, Fujian Institute of Research on the Structure of Matter, The Chinese Academy of Sciences, Fuzhou, Fujian 350002, China, and Graduate School of the Chinese Academy of Sciences, Beijing 100039, China

Received July 7, 2007

A family of manganese complexes, $[Mn_5O_3(t\text{-}BuPO_3)_2(MeCOO)_5(H_2O)(phen)_2]$ (**1**), $[Mn_5O_3(t\text{-}BuPO_3)_2(PhCOO)_5(phen)_2]$ (**2**), $[Mn_4O_2(t\text{-}BuPO_3)_2(RCOO)_4(bpy)_2]$ (R = Me, (**3**); R = Ph, (**4**)), $NBu^n{}'_4[Mn_4O_2(EtCOO)_3(MeCOO)_4(pic)_2]$ (**5**), $NR'_4[Mn_4O_2(i\text{-}PrCOO)_7(pic)_2]$ (R′ = Bu^n, (**6**); R′ = Et, (**7**)), were synthesized and characterized. The seven manganese clusters were all prepared from a reaction system containing *tert*-butylphosphonic acid, $Mn(O_2CR)_2$ (R = Me, Ph) and NR'_4MnO_4 (R′ = Bu^n, Et) with similar procedures except for using different N-containing ligands (1,10-phenanthroline (phen), 2,2′-bipyridine (bpy) and picolinic acid (picH)) as coligands. The structures of these complexes vary with the N-containing donors. Both the cores of complexes **1** and **2** feature three μ_3-O and two capping $t\text{-}BuPO_3^{2-}$ groups bridging five Mn^{III} atoms to form a basket-like cage structure. Complexes **3** and **4** both have one $[Mn_4(\mu_3\text{-}O)_2]^{8+}$ core with four coplanar Mn^{III} atoms disposed in an extended "butterfly-like" arrangement and two capping $\mu_3\text{-}t\text{-}BuPO_3^{2-}$ binding to three manganese centers above and below the Mn_4 plane. Complexes **5**, **6**, and **7** all possess one $[Mn_4(\mu_3\text{-}O)_2]^{8+}$ core just as complexes **3** and **4**, but they display a folded "butterfly-like" conformation with the four Mn^{III} atoms nonplanar. Thus, the seven compounds are classified into three types, and three representative compounds **1 · 2H$_2$O · MeOH · MeCN**, **3 · 6H$_2$O · 2MeCOOH**, and **5 · 0.5H$_2$O** have been characterized by IR spectroscopy, ESI-MS spectroscopy, magnetic measurements and *in situ* UV−vis−NIR spectroelectrochemical analysis. Magnetic susceptibility measurements reveal the existence of both ferromagnetic and antiferromagnetic interactions between the adjacent Mn^{III} ions in compound **1 · 2H$_2$O · MeOH · MeCN**, and antiferromagnetic interactions in **3 · 6H$_2$O · 2MeCOOH** and **5 · 0.5H$_2$O.** Fitting the experimental data led to the following parameters: $J_1 = -2.18$ cm^{-1}, $J_2 = 6.93$ cm^{-1}, $J_3 = -13.94$ cm^{-1}, $J_4 = -9.62$ cm^{-1}, $J_5 = -11.17$ cm^{-1}, $g = 2.00$ (**1 · 2H$_2$O · MeOH · MeCN**), $J_1 = -5.41$ cm^{-1}, $J_2 = -35.44$ cm^{-1}, $g = 2.13$, $zJ' = -1.55$ cm^{-1} (**3 · 6H$_2$O · 2MeCOOH**) and $J_1 = -2.29$ cm^{-1}, $J_2 = -35.21$ cm^{-1}, $g = 2.02$, $zJ' = -0.86$ cm^{-1} (**5 · 0.5H$_2$O**).

Introduction

Manganese complexes are attracting considerable interest in recent years in the fields of bioinorganic chemistry and magnetic materials. It is generally accepted that a tetranuclear manganese cluster resides at the active site of Photosystem II in green plants to catalyze the light-driven water oxidation reaction to generate dioxygen.[1–3] The synthesis and structure characterization of manganese complexes have provided a wealth of data to model the photosynthetic water oxidation center.[4] On the other hand, the magnetic behavior of manganese clusters makes them have potential application in the design of molecular magnetic materials, which has been of considerable interest.[5–9] Over the past several years,

* To whom correspondence should be addressed. E-mail: ccn@fjirsm.ac.cn.
† Fujian Institute of Research on the Structure of Matter, The Chinese Academy of Sciences.
‡ Graduate School of the Chinese Academy of Sciences.

(1) Mukhopadhyay, S.; Mandal, S. K.; Bhaduri, S.; Armstrong, W. H. *Chem. Rev.* **2004**, *104*, 3981.
(2) Photosynthetic water oxidation: Special Dedicated Issue, Nugent, J., Ed.; *Biochim. Biophys. Acta* **2001**, *1503*, 1.

10.1021/ic701343s CCC: $40.75
Published on Web 06/10/2008

a number of manganese clusters have been reported.[3,4,10] So far, the common strategy to prepare polynuclear manganese complexes relies mostly on the use of the carboxylate ligand, and the manganese carboxylate chemistry has been explored extensively by Christou et al.[4a,d,e,g,m,10a–c,11] To synthesize new polynuclear manganese species, we have tried to develop new synthetic routes and oriented our research strategy to the use of phosphonates to substitute some of the carboxylate ligands.

Phosphonates are a family of ligands in possession of three O donors that can bind to more than one metal ion simultaneously. Transition-metal phosphonate complexes have received a lot of attention in recent years primarily because of their potential applications in catalysis, ion exchange, proton conductivity, intercalation chemistry, photochemistry, and material chemistry.[12–15] Several polynuclear metal phosphonate compounds that contain vanadium,[16] aluminum,[17] copper,[18] cobalt,[19] zinc,[20] cadmium,[21] and iron[22] have been prepared so far. Recently utilization of the phosphonate to prepare manganese complexes has received increasing attention, and several types of target clusters with higher nuclearity, such as hexa-, icosa-, dodeca-, trideca- and docosa- nuclear manganese aggregates have been obtained.[19,23–27] However, smaller manganese clusters, for example, the pentanuclear and tetranuclear manganese complexes with phosphonate ligands remain relatively scarce.[28] For the reasons above, we have fully explored the reaction system containing *tert*-butylphosphonic acid and successfully obtained a family of manganese clusters with lower nuclearity: $[Mn_5O_3(t\text{-}BuPO_3)_2(MeCOO)_5H_2O(phen)_2]$ (**1**), $[Mn_5O_3(t\text{-}BuPO_3)_2(PhCOO)_5(phen)_2]$ (**2**), $[Mn_4O_2(t\text{-}BuPO_3)_2(RCOO)_4(bpy)_2]$ (R = Me, (**3**); R = Ph, (**4**)), $NBu^n_4[Mn_4O_2(EtCOO)_3(MeCOO)_4(pic)_2]$ (**5**), $NR'_4[Mn_4O_2(i\text{-}PrCOO)_7(pic)_2]$ (R′ = Bu^n, (**6**); R′ = Et, (**7**)). Herein the synthesis, structures, magnetic properties, and electrochemistry of these complexes are presented.

Experimental Section

Syntheses. All manipulations were performed under aerobic condition. $Mn(O_2CPh)_2\cdot 2H_2O$[4d] and $NBu^n_4MnO_4$[29] were both prepared according to the literature. NEt_4MnO_4 was prepared in a

(3) (a) Hanley, J.; Sarrou, J.; Petrouleas, V. *Biochemistry* **2000**, *39*, 15441. (b) Zheng, M.; Dismukes, G. C. *Inorg. Chem.* **1996**, *35*, 3307. (c) Kulik, L. V.; Epel, B.; Lubitz, W.; Messinger, J. *J. Am. Chem. Soc.* **2005**, *127*, 2392. (d) Yachandra, V. K.; Sauer, K.; Klein, M. P. *Chem. Rev.* **1996**, *96*, 2927. (e) Koulougliotis, D.; Shen, J.-R.; Ioannidis, N.; Petrouleas, V.;. *Biochemistry* **2003**, *42*, 3045. (f) Peloquin, J. M.; Campbell, K. A.; Randall, D. W.; Evanchik, M. A.; Pecoraro, V. L.; Armstrong, W. H.; Britt, R. D. *J. Am. Chem. Soc.* **2000**, *122*, 10926. (g) de Paula, J. C.; Beck, W. F.; Brudvig, G. W. *J. Am. Chem. Soc.* **1986**, *108*, 4002. (h) Hasegawa, K.; Ono, T. A.; Inoue, Y.; Kusunoki, M. *Chem. Phys. Lett.* **1999**, *300*, 9. (i) Randall, D. W.; Sturgeon, B. E.; Ball, J. A.; Lorigan, G. A.; Chan, M. K.; Klein, M. P.; Armstrong, W. H.; Britt, R. D. *J. Am. Chem. Soc.* **1995**, *117*, 11780. (j) McEvoy, J. P.; Brudvig, G. W. *Chem. Rev.* **2006**, *108*, 4455.

(4) (a) Wang, S.; Tsai, H.-L.; Libby, E.; Folting, K.; Streib, W. E.; Hendrickson, D. N.; Christou, G. *Inorg. Chem.* **1996**, *35*, 7578. (b) Philouze, C.; Blondin, G.; Girerd, J.-J.; Guilhem, J.; Pascard, C.; Lexa, D. *J. Am. Chem. Soc.* **1994**, *116*, 8557. (c) Chan, M. K.; Armstrong, W. H. *J. Am. Chem. Soc.* **1990**, *112*, 4985. (d) Libby, E.; McCusker, J. K.; Schmitt, E. A.; Folting, K.; Hendrickson, D. N.; Christou, G. *Inorg. Chem.* **1991**, *30*, 3486. (e) Wemple, M. W.; Tsai, H.-L.; Folting, K.; Hendrickson, D. N.; Christou, G. *Inorg. Chem.* **1993**, *32*, 2025. (f) Kirk, M. L.; Chan, M. K.; Armstrong, W. H.; Solomon, E. I. *J. Am. Chem. Soc.* **1992**, *114*, 10432. (g) Wemple, M. W.; Adams, D. M.; Folting, K.; Hendrickson, D. N.; Christou, G. *J. Am. Chem. Soc.* **1995**, *117*, 7275. (h) Ruettinger, W. F.; Campana, C.; Dismukes, G. C. *J. Am. Chem. Soc.* **1997**, *119*, 6670. (i) Dubé, C. E.; Wright, D. W.; Pal, S.; Bonitatebus, P. J.; Armstrong, W. H. *J. Am. Chem. Soc.* **1998**, *120*, 3704. (j) Gedye, C.; Harding, C.; McKee, V.; Nelson, J.; Patterson, J. *J. Chem. Soc., Chem. Commun.* **1992**, 392. (k) Chandra, S. K.; Chakraborty, P.; Chakravorty, A. *J. Chem. Soc., Dalton Trans.* **1993**, 863. (l) Wang, S.; Folting, K.; Streib, W. E.; Schmitt, E. A.; McCusker, J. K.; Hendrickson, D. N.; Christou, G. *Angew. Chem., Int. Ed. Engl.* **1991**, *30*, 305. (m) Vincent, J. B.; Christmas, C.; Chang, H.-R.; Li, Q.; Boyd, P. D. W.; Huffman, J. C.; Hendrickson, D. N.; Christou, G. *J. Am. Chem. Soc.* **1989**, *111*, 32086.

(5) Kahn, O. *Molecular Magnetism*; VCH: New York, 1993.

(6) *Magnetism: Molecules to Materials*; Miller, J. S., Drilon, M., Eds.; Wiley-VCH: Weinheim, Germany, 2002.

(7) Gatteschi, D.; Sessoli, R. *Angew. Chem., Int. Ed.* **2003**, *42*, 268.

(8) Tejada, J.; Chudnovsky, E. M.; del Barco, E.; Hernandez, J. M.; Spiller, T. P. *Nanotechnology* **2001**, *12*, 181.

(9) Zhou, B.; Tao, R.; Shen, S.-Q.; Liang, J.-Q. *Phys. Rev. A* **2002**, 66, 010301(R)

(10) (a) Cañada-Vilalta, C.; Streib, W. E.; Huffman, J. C.; O'Brien, T. A.; Davidson, E. R.; Christou, G. *Inorg. Chem.* **2004**, *43*, 101. (b) Milios, C. J.; Vinslava, A.; Wernsdorfer, W.; Moggach, S.; Parsons, S.; Perlepes, S. P.; Christou, G.; Brechin, E. K. *J. Am. Chem. Soc.* **2007**, *129*, 2754. (c) Harden, C. N.; Bolcar, M. A.; Wernsdorfer, W.; Abboud, K. A.; Streib, W. E.; Christou, G. *Inorg. Chem.* **2003**, *42*, 7067. (d) Milios, C. J.; Vinslava, A.; Whittaker, A. G.; Parsons, S.; Wernsdorfer, W.; Christou, G.; Perlepes, S. P.; Brechin, E. K. *Inorg. Chem.* **2006**, *45*, 5272. (e) Lecren, L.; Wernsdorfer, W.; Li, Y.-G.; Vindigni, A.; Miyasaka, H.; Clérac, R. *J. Am. Chem. Soc.* **2007**, *129*, 5045.

(11) (a) Sessoli, R.; Gatteschi, D.; Caneschi, A.; Novak, M. A. *Nature* **1993**, *365*, 414. (b) Hill, S.; Edwards, R. S.; Aliaga-Alcalde, N.; Christou, G. *Science* **2003**, *302*, 1015. (c) Miyasaka, H.; Clérac, R.; Wernsdorfer, W.; Lecren, L.; Bonhomme, C.; Sugiura, K.; Yamashita, M. *Angew. Chem., Int. Ed.* **2004**, *43*, 2801. (d) Mishra, A.; Wernsdorfer, W.; Abboud, K. A.; Christou, G. *J. Am. Chem. Soc.* **2004**, *126*, 15648. (e) Aubin, S. M. J.; Wemple, M. W.; Adams, D. M.; Tsai, H.-L.; Christou, G.; Hendrickson, D. N. *J. Am. Chem. Soc.* **1996**, *118*, 7746.

(12) Song, S. Y.; Ma, J. F.; Yang, J.; Cao, M. H.; Li, K. C. *Inorg. Chem.* **2005**, *44*, 2140.

(13) Bujoli, B.; Lane, S. M.; Nonglaton, G.; Pipelier, M.; Léger, J.; Talham, D. R.; Tellier, C. *Chem.—Eur. J.* **2005**, *11*, 1980.

(14) Maeda, K. *Microporous Mesoporous Mater.* **2004**, *73*, 47.

(15) Cheetham, A. K.; Férey, G.; Loiseau, T. *Angew. Chem., Int. Ed.* **1999**, *38*, 3268.

(16) Khan, M. I.; Zubieta, J. *Prog. Inorg. Chem.* **1995**, *43*, 1, and references therein.

(17) Walawalkar, M. G.; Roesky, H. W.; Murugavel, R. *Acc. Chem. Res.* **1999**, *32*, 117, and references therein.

(18) Chandrasekhar, V.; Kingsley, S. *Angew. Chem., Int. Ed.* **2000**, *39*, 2320.

(19) Brechin, E. K.; Coxall, R. A.; Parkin, A.; Parsons, S.; Tasker, P. A.; Winpenny, R. E. P. *Angew. Chem., Int. Ed.* **2001**, *40*, 2700.

(20) Chandrasekhar, V.; Kingsley, S.; Rhatigan, B.; Lam, M. K.; Rheingold, A. L. *Inorg. Chem.* **2002**, *41*, 1030.

(21) Anantharaman, G.; Walawalker, M. G.; Murugavel, R.; Gabor, B.; Herbst-Irmer, R.; Baldus, M.; Angerstein, B.; Roesky, H. W. *Angew.Chem., Int. Ed.* **2003**, *42*, 4482.

(22) Tolis, E. I.; Helliwell, M.; Langley, S.; Raftery, J.; Winpenny, R. E. P. *Angew. Chem., Int. Ed.* **2003**, *42*, 3804.

(23) Maheswaran, S.; Chastanet, G.; Teat, S. J.; Mallah, T.; Sessoli, R.; Wernsdorfer, W.; Winpenny, R. E. P. *Angew. Chem., Int. Ed.* **2005**, *44*, 5044.

(24) Yao, H.-C.; Li, Y.-Z.; Song, Y.; Ma, Y.-S.; Zheng, L.-M.; Xin, X.-Q. *Inorg. Chem.* **2006**, *45*, 59.

(25) Ma, Y.-S.; Song, Y.; Li, Y.-Z.; Zheng, L.-M. *Inorg. Chem.* **2007**, *46*, 5459.

(26) Shanmugam, M.; Chastanet, G.; Mallah, T.; Sessoli, R.; Teat, S. J.; Timco, G. A.; Winpenny, R. E. P. *Chem.—Eur. J.* **2006**, *12*, 8777.

(27) Shanmugam, M.; Shanmugam, M.; Chastanet, G.; Sessoli, R.; Mallah, T.; Wernsdorfer, W.; Winpenny, R. E. P. *J. Mater. Chem.* **2006**, *16*, 2576.

(28) (a) Baslar, V.; Shanmugam, M.; Sañudo, E. C.; Shanmugam, M.; Collison, D.; Mclnnes, E. J. L.; Wei, Q.; Winpenny, R. E. P. *Chem. Commun.* **2007**, *1*, 37. (b) Wang, M.; Ma, C.; Yuan, D.; Hu, M.; Chen, C.; Liu, Q. *New J. Chem.* **2007**, *31*, 2103. (c) Ma, Y.-S.; Yao, H.-C.; Hua, W.-J.; Li, S.-H.; Li, Y.-Z.; Zheng, L.-M. *Inorg. Chim. Acta* **2007**, *360*, 1645.

(29) Sala, T.; Sargent, M. V. *J. Chem. Soc., Chem. Commun.* **1978**, 253.

similar manner with $NBu^n_4MnO_4$.[30] All the other chemical reagents and solvents were of analytical grade, were purchased commercially, and were used without further purification.

$[Mn_5O_3(t\text{-}BuPO_3)_2(MeCOO)_5(H_2O)(phen)_2]\cdot 2H_2O\cdot MeOH\cdot MeCN$ ($1\cdot 2H_2O\cdot MeOH\cdot MeCN$). To a stirred solution of $Mn(O_2CMe)_2\cdot 4H_2O$ (0.245 g, 1 mmol) and MeCOOH (7 mL, 0.122 mol) in MeCN (15 mL) was added solid $NBu^n_4MnO_4$ (0.091 g, 0.25 mmol) in small portions. To the resulting brown solution was added a solution of 1,10-phenanthroline (0.10 g, 0.5 mmol) and *tert*-butylphosphonic acid (*t*-$BuPO_3H_2$) (0.070 g, 0.5 mmol) in MeOH (5 mL) to yield a dark brown solution which was stirred for 24 h at room temperature and then filtered. The filtrate was left to stand at room temperature for about 1 week, during which time brown crystals were produced in 21% yield based on Mn. Anal. Calcd (%) for $C_{45}H_{62}Mn_5N_5O_{23}P_2$: C, 39.20; H, 4.50; N, 5.08. Found: C, 39.15; H, 4.53; N, 5.12. Selected IR (KBr, cm^{-1}) data: 3417 (s), 1581 (s), 1518 (s), 1407 (s), 1102 (w), 976 (m), 725 (w).

$[Mn_5O_3(t\text{-}BuPO_3)_2(PhCOO)_5(phen)_2]\cdot H_2O\cdot MeCN$ ($2\cdot H_2O\cdot MeCN$). This complex was obtained using a procedure similar to that used for preparing **$1\cdot 2H_2O\cdot MeOH\cdot MeCN$**, except that $Mn(O_2CPh)_2\cdot 2H_2O$ was used instead of $Mn(O_2CMe)_2\cdot 4H_2O$, PhCOOH instead of MeCOOH, and CH_2Cl_2/MeCN (v/v 2:1, 15 mL) instead of MeCN (15 mL). The brown crystals were produced in 17% yield based on Mn. Anal. Calcd (%) for $C_{69}H_{64}Mn_5N_5O_{20}P_2$: C, 51.11; H, 3.95; N, 4.32. Found: C, 51.04; H, 3.83; N, 4.63. Selected IR (KBr, cm^{-1}) data: 3413 (s), 1600 (s), 1518 (s), 1384 (s), 1099 (w), 973 (m), 719 (w).

$[Mn_4O_2(t\text{-}BuPO_3)_2(MeCOO)_4(bpy)_2]\cdot 6H_2O\cdot 2MeCOOH$ ($3\cdot 6H_2O\cdot 2MeCOOH$). The synthetic procedure of **$1\cdot 2H_2O\cdot MeOH\cdot MeCN$** was utilized to prepare **$3\cdot 6H_2O\cdot 2MeCOOH$** with the use of 2,2′-bipyridine in place of 1,10-phenanthroline. The brown crystals were produced in 26% yield based on Mn. Anal. Calcd (%) for $C_{40}H_{66}Mn_4N_4O_{26}P_2$: C, 36.90; H, 5.07; N, 4.31. Found: C, 36.74; H, 5.02; N, 4.53. Selected IR (KBr, cm^{-1}) data: 3479 (s), 2966 (w), 1703 (m), 1575 (s), 1399 (s), 1342 (w), 979 (w), 943 (m), 665 (m).

$[Mn_4O_2(t\text{-}BuPO_3)_2(PhCOO)_4(bpy)_2]\cdot H_2O\cdot 3PhCOOH$($4\cdot H_2O\cdot 3PhCOOH$). This complex was obtained using a procedure similar to that used for preparing **$2\cdot H_2O\cdot MeCN$,** except that 2,2′-bipyridine was used instead of 1,10-phenanthroline. The brown crystals were produced in 21% yield based on Mn. Anal. Calcd (%) for $C_{77}H_{72}Mn_4N_4O_{23}P_2$: C, 54.25; H, 4.23; N, 3.29. Found: C, 54.12; H, 4.47; N, 3.45. Selected IR (KBr, cm^{-1}) data: 3479 (s), 2966 (w), 1703 (m), 1575 (s), 1399 (s), 1342 (w), 979 (w), 943 (m), 665 (m).

$NBu^n_4[Mn_4O_2(EtCOO)_3(MeCOO)_4(pic)_2]\cdot 0.5H_2O$ ($5\cdot 0.5H_2O$). This complex was obtained using a procedure similar to that used for preparing **$1\cdot 2H_2O\cdot MeOH\cdot MeCN$**, except that picolinic acid was used instead of 2,2′-bipyridine, EtCOOH instead of MeCOOH. The brown crystals were produced in 29% yield based on Mn. Anal. Calcd (%) for $C_{45}H_{71}Mn_4N_3O_{20.5}$: C, 44.93; H, 5.91; N, 3.49. Found: C, 44.89; H, 5.63; N, 3.74. Selected IR (KBr, cm^{-1}) data: 3452 (m), 2965 (m), 1676 (s), 1464 (w), 1398 (s), 1331 (s), 1284 (m), 649 (m).

$NBu^n_4[Mn_4O_2(i\text{-}PrCOO)_7(pic)_2]$ (6). This complex was obtained using a procedure similar to that used for preparing **$5\cdot 0.5H_2O$**, except that *i*-PrCOOH was used instead of EtCOOH. The brown crystals were produced in 20% yield based on Mn. Anal. Calcd (%) for $C_{56}H_{93}Mn_4N_3O_{20}$: C, 49.85; H, 6.90; N, 3.12. Found: C, 49.78; H, 6.79; N, 3.31. Selected IR (KBr, cm^{-1}) data: 2967 (m), 1583 (s), 1446 (m), 1399 (s), 1337 (w), 1015 (w), 943 (m), 665 (w).

$NEt_4[Mn_4O_2(i\text{-}PrCOO)_7(pic)_2]\cdot 0.5H_2O$ ($7\cdot 0.5H_2O$). This complex was obtained using a procedure similar to that used for preparing **6**, except that NEt_4MnO_4 was used instead of $NBu^n_4MnO_4$. The brown crystals were produced in 19% yield based on Mn. Anal. Calcd (%) for $C_{48}H_{78}Mn_4N_3O_{20.5}$: C, 46.27; H, 6.26; N, 3.37. Found: C, 46.21; H, 6.39; N, 3.24. Selected IR (KBr, cm^{-1}) data: 3452 (m), 2967 (w), 1682 (m), 1602 (s), 1406 (s), 1331 (w), 1275 (m), 1094 (w), 676 (w).

Physical Measurements. Elemental analyses (carbon, hydrogen, and nitrogen) were performed using a vario EL III CHNOS elemental analyzer. Infrared spectra were recorded on a Nicolet magna 750 FT-IR spectrophotometer using KBr pellets in the range of 400∼4000 cm^{-1}. Electrospray mass spectra were recorded with a DECAX-30000 LCQ Deca XP mass spectrometer. Electrochemical studies were performed by a CHI630A voltammetric analyzer. The auxiliary electrode was a Pt wire, the reference electrode a Ag/AgCl electrode, and the working electrode a glassy carbon disk, which was carefully polished with gamma alumina powder (0.05 μm) before each voltammogram and then washed carefully with distilled dichloromethane. *In situ* UV−vis−NIR absorption spectra were recorded in a Varian Cary500 spectrophotometer coupled to a potentiostat using a quartz glass cuvette as spectroelectrochemical cell. The measurement was recorded at room temperature in distilled CH_2Cl_2 solution under argon and 0.1 M $NBu^n_4PF_6$ was added as supporting electrolyte. The variable-temperature magnetic susceptibility (2−300 K) was measured with a model PPMS60000 superconducting extraction sample magnetometer under a field of 0.5 T with the crystalline sample kept in a capsule for weighing.

X-ray Crystallography. The diffraction data for the seven complexes were collected at 293(2) K on a mercury-CCD/AFCR diffractometer with Mo Kα radiation (λ = 0.71073 Å). Single crystals were in all cases selected under a microscope and then attached to the tip of glass capillaries with grease. The empirical absorption correction was applied by using the SADABS program.[31] All the structures were solved by direct methods and refined by full-matrix least-squares techniques based on $F^2$with all observed reflections performed with the SHELXTL-97 package.[32] The non-hydrogen atoms were refined anisotropically. The hydrogen atoms were located by geometrical calculations except for those on the water molecules which were located from the difference Fourier syntheses. The SQUEEZE[33] instruction in the PLATON software[34] was applied to treat the raw data for the cation of compound **6**. Details of the crystal data and structure refinement of the seven compounds are listed in Table 1.

Results and Discussion

Synthesis. The ability of phosphonic acid ligands to support various structures is well demonstrated by the growing number of reports on phosphonate clusters.[16–28] During our investigation, we have explored the reaction system of *tert*-butylphosphonic acid with manganese salts ($Mn(O_2CR)_2$ (R = Me, Ph)) in combination with the

(30) Karaman, H.; Barton, R. J.; Robertson, B. E.; Lee, D. G. *J. Org. Chem.* **1984**, *49* (23), 4509.

(31) Sheldrick, G. M. *SADABS Software for Empirical Absorption Correction*; University of Göttingen: Göttingen, Germany, 1996.

(32) Sheldrick, G. M. *SHELXTL, Structure Determination Software Programs*; Bruker Analytical X-ray System Inc: Madison, WI, 1997.

(33) SQUEEZE: Sluis, P. v. d.; Spek, A. L. *Acta Crystallogr., Sect. A* **1990**, *46*, 194.

(34) PLATON software: Spek, A. L. *A Multipurpose Crystallographic Tool*; Utrecht University: Utrecht, The Netherlands, 1998.

Table 1. Crystallographic Data for Complexes **1**−**7**

	complex		
	1·2H$_2$O·MeOH·MeCN	**2**·H$_2$O·MeCN	**3**·6H$_2$O·2MeCOOH
formula[a]	$C_{45}H_{62}Mn_5N_5O_{23}P_2$	$C_{69}H_{64}Mn_5N_5O_{20}P_2$	$C_{40}H_{66}Mn_4N_4O_{26}P_2$
space group	$P\bar{1}$	$P2_1/c$	$P\bar{1}$
fw	1377.64	1619.89	1300.67
a, Å	12.1843(4)	13.939(5)	10.652(4)
b, Å	15.2634(9)	19.425(8)	11.931(4)
c, Å	17.0702(7)	29.166(12)	13.295(5)
α, deg	82.720(9)	90	115.296(4)
β, deg	81.662(9)	94.515(10)	90.36
γ, deg	79.114(8)	90	113.407(4)
V, Å^3	3068.4(2)	7873(5)	1370.0(9)
Z	2	4	1
T, K	293(2)	293(2)	293(2)
λ, Å[b]	0.71073	0.71073	0.71073
ρ_{calcd}, g cm^{-3}	1.491	1.367	1.577
μ, mm^{-1}	1.129	0.889	1.046
R_1[c]	0.0788	0.0707	0.0368
wR_2[d]	0.1934	0.2022	0.0838

	complex			
	4·H$_2$O·3PhCOOH	**5**·0.5H$_2$O	**6**	**7**·0.5H$_2$O
formula[a]	$C_{77}H_{72}Mn_4N_4O_{23}P_2$	$C_{45}H_{71}Mn_4N_3O_{20.5}$	$C_{56}H_{93}Mn_4N_3O_{20}$	$C_{48}H_{78}Mn_4N_3O_{20.5}$
space group	$P2_1/c$	$P\bar{1}$	$P\bar{1}$	$P2_1/c$
fw	1703.09	1201.81	1348.09	1244.89
a, Å	14.308(2	12.575(5	12.617(12)	12.221(4)
b, Å	13.0663(18)	12.724(5)	13.145(12)	21.229(6)
c, Å	23.021(3)	19.455(8)	21.89(2)	23.495(7)
α, deg	90	78.848(9)	89.67(2)	90
β, deg	106.091(4)	84.450(8)	86.989(15)	104.561(3)
γ, deg	90	83.593(11)	85.51(2)	90
V, Å^3	4135.1(10)	3026(2)	3615(6)	5900(3)
Z	2	2	2	4
T, K	293(2)	293(2)	293(2)	293(2)
λ, Å[b]	0.71073	0.71073	0.71073	0.71073
ρ_{calcd}, g cm^{-3}	1.368	1.317	1.238	1.429
μ, mm^{-1}	0.709	0.883	0.746	0.912
R_1[c]	0.0609	0.0733	0.0928	0.0995
wR_2[d]	0.165	0.2014	0.1686	0.2160

[a] Including solvent molecules. [b] Graphite monochromator. [c] $R_1 = \sum(||F_o| - |F_c||)/\sum|F_o|$. [d] w$R_2 = [\sum w(F_o^2 - F_c^2)^2/\sum w(F_o^2)^2]^{0.5}$.

N-containing ligands (phen, bpy, and picH). It is interesting to note that compounds **1**−**7** were all prepared in similar one-port procedures which lead to three species of complexes. Previous work had proved that NR′$_4$MnO$_4$ (R′ = Bu^n, Et) in nonaqueous solvents represents a useful route to forming higher oxidation state Mn complexes.[35,36] The seven compounds **1**−**7** were all prepared from the comproportionation reactions between Mn^{II} and NR′$_4$MnO$_4$ (R′ = Bu^n, Et) which resulted in the average Mn oxidation state of +3 in all of the seven compounds. Complexes **1** and **2** contain a novel [Mn$_5$O$_3$] core, which has not yet been reported so far, though several pentanuclear manganese(II),[37,38] manganese(III),[39] and mixed valent manganese(II and III)[40–42] clusters have been prepared before. It is worthwhile to point out that the participation of the N-containing coligands (bpy, phen, pyridine, etc.) seems necessary to obtain the polynuclear Mn phosphonate clusters in spite of the various synthetic procedures when we read throughout all the synthetic reports on the polynuclear Mn phosphonate clusters. With the variation of the N-containing coligand, a variety of structures with higher nuclearity were obtained for the Mn phosphonate cluster family. In this work, the use of phen has led to a novel Mn$_5$O$_3$ cluster while the use of bpy in place of phen in the same ratio and in the similar reaction system has led to a completely different kind of complex [Mn$_4$O$_2$(*t*-BuPO$_3$)$_2$(RCOO)$_4$(bpy)$_2$] (R = Me, (**3**); R = Ph, (**4**)). Whereas, when picH was used instead of phen, a known type of the complex NBu$^n_4$[Mn$_4$O$_2$(MeCOO)$_7$(pic)$_2$][4d] was obtained, and the *tert*-butylphosphonate group failed to ligate to the manganese ion. It is considered that in contrast with the basicity of phen and bpy, the acidity of picolinic acid will be unfavorable for the total deprotonation of *tert*-butylphosphonic acid while the deprotonation should be important for tridentate coordination of the alkylphosphonate. It is also noticed that as a dibasic acid, alkylphosphonic acid has its pK_1 = 2.8 and pK_2 = 8.4[43] implying that the total deprotonation would be difficult in the presence of picolinic

(35) Vincent, J. B.; Chang, H.-R.; Folting, K.; Huffman, J. C.; Christou, G.; Hendrickson, D. N. *J. Am. Chem. Soc.* **1987**, *109*, 5703.
(36) Bouwman, E.; Bolcar, M. A.; Libby, E.; Huffman, J. C.; Folting, K.; Christou, G. *Inorg. Chem.* **1992**, *31*, 5185.
(37) Matthews, C. J.; Thompson, L. K.; Parsons, S. R.; Xu, Z.; Miller, D. O.; Heath, S. L. *Inorg. Chem.* **2001**, *40*, 4448.
(38) Matthews, C. J.; Xu, Z.; Mandal, S. K.; Thompson, L. K.; Biradha, K.; Poirier, K.; Zaworotko, M. J. *Chem. Commun.* **1999**, 347.
(39) Reynolds, R. A., III; Coucouvanis, D. *Inorg. Chem.* **1998**, *37*, 170.
(40) Lah, M. S.; Pecoraro, V. L. *J. Am. Chem. Soc.* **1989**, *111*, 7258.
(41) Berlinguette, C. P.; Vaughn, D.; Cañada-Vilalta, C.; Galán-Mascarós, R. G.; Dunbar, K. R. *Angew. Chem., Int. Ed.* **2003**, *42*, 1523.
(42) Yang, C.-I.; Wernsdorfer, W.; Lee, G.-H.; Tsai, H.-L. *J. Am. Chem. Soc.* **2007**, *129*, 456.

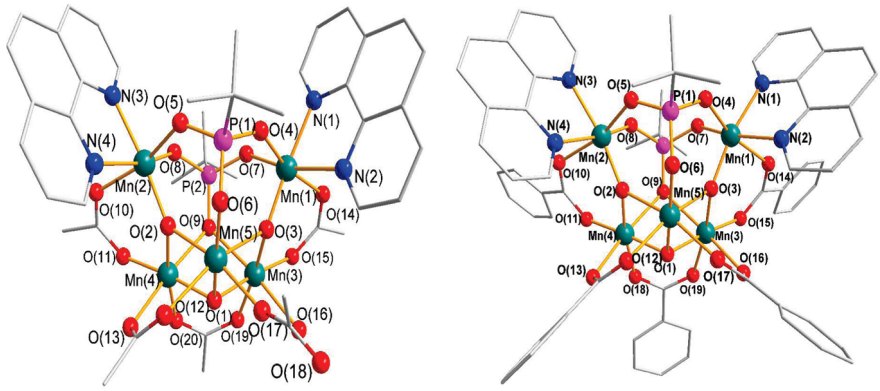

Figure 1. DIAMOND view of (a) compound **1** and (b) compound **2**. Hydrogen atoms have been omitted for clarity.

acid with pK = 5.32.[44] Consequently it is comprehensible that despite many attempts, we failed to introduce *tert*-butylphosphonate into the manganese compounds in the reaction system containing picH and just obtained the Mn_4O_2 carboxylate complexes **5**, **6**, and **7**. Interestingly, complex **5** contains mixed aliphatic carboxylate ligands in its Mn_4O_2 core, which is the first example of the family. It is considered that EtCOOH exhibits similar acidity and structural features to those of acetic acid; therefore, the substitution of $EtCOO^-$ for AcO^- is likely incomplete and leads to mixed aliphatic carboxylate ligands in complex **5**.

Description of Crystal Structures

$[Mn_5O_3(t\text{-}BuPO_3)_2(MeCOO)_5(H_2O)(phen)_2]$ (1) and $[Mn_5O_3(t\text{-}BuPO_3)_2(PhCOO)_5(phen)_2]$ (2). The molecular structure of complex **1** is shown in Figure 1a, while selected bond distances and angles of **1** are listed in Table 2.

Complex **1** possesses a pentanuclear core $[Mn_5O_3]^{9+}$ and the five manganese atoms are all in +3 oxidation state according to the bond valence sum calculations.[45] The peripheral ligation is composed of two t-$BuPO_3^{2-}$, five $MeCOO^-$, one H_2O, and two terminal phen groups. The two *tert*-butylphosphonate ligands in **1** adopt two kinds of binding mode: [4.211] and [3.111] by the Harris notation (Scheme 1).[46]

Five manganese atoms are bridged by three μ_3-O and two t-$BuPO_3^{2-}$ to form an unprecedented basket-like cage structure (Figure 2). The Mn(3), Mn(4), Mn(5) atoms with intermanganese bond lengths of Mn(3)···Mn(4), 2.9928(12); Mn(4)···Mn(5), 2.8442(13); Mn(3)···Mn(5), 2.9892(12) (Å) are linked by μ_3-O(1) forming a cone-shaped bottom of the basket. And the mouth of the basket is composed of the eight-membered ring of {Mn(1)−O(4)−P(1)−O(5)−Mn(2)−O(8)−P(2)−O(7)}. Unlike the Mn_3O complexes,[35,47,48] the three μ_3-O atoms O(1), O(2), O(3) are not in the three triangular planes made up of {Mn(3), Mn(4), Mn(5)}, {Mn(2), Mn(4), Mn(5)}, and {Mn(1), Mn(3), Mn(5)} but outside of the planes by 0.8150, 0.2018, and 0.3305 Å, respectively. The five manganese atoms are all six-coordinate with near-octahedral geometry around each center. The Mn(1) and Mn(2) atoms are each surrounded by two phosphonate oxygen atoms, one μ_3-O, one acetate oxygen atom, and two 1,10-phenanthroline nitrogens. The Mn(4) and Mn(5) atoms are both coordinated by one phosphonate oxygen atom, two μ_3-O, and three acetate oxygen atoms. It is notable that the coordination environment of Mn(3) is slightly different from that of Mn(4) and Mn(5) in that one oxygen atom (O(16)) from the H_2O molecule chelates to Mn(3) instead of the acetate oxygen atom. One acetate group is monodentate, and O(18) of the acetate group is not involved in manganese coordination. The average distance of $Mn-O_{phosphonate}$ is 2.048(4) Å which is comparable with that reported for manganese phosphonates.[19,23,24]

As shown in Figures 1b and 2, complex **2** possesses analogous molecular structure to that of **1** and the identical inorganic core structure with **1**. However, the peripheral ligation of complex **2** consists of two t-$BuPO_3^{2-}$, six $PhCOO^-$, and two terminal phen groups, of which the six $PhCOO^-$ are all bidentate bridges and no H_2O is coordinated to Mn. A comparison of selected bonds distances and angles of **1** with those of **2** is given in Supporting Information, Table S1.

$[Mn_4O_2(t\text{-}BuPO_3)_2(RCOO)_4(bpy)_2]$ (R = Me, (3); R = Ph, (4)). The Oak Ridge Thermal Ellipsoid Plot (ORTEP) diagram for complex **3** is illustrated in Figure 3a, while selected bond lengths and angles for **3** are given in Table 3. Complex **3** crystallizes in triclinic $P\bar{1}$ space group with C_{2v} symmetry. It possesses an $[Mn_4(\mu_3\text{-}O)_2]^{8+}$ core with the four coplanar Mn atoms disposed in an extended "butterfly-like" arrangement which is similar to that in the previously reported $[Mn_4(\mu_3\text{-}O)_2]^{8+}$ complexes.[49,50] However, there are two capping *tert*-butylphosphonate ligands above and below the core, which is markedly different from the reported Mn_4

(43) White, J. R. *J. Am. Chem. Soc.* **1950**, *72*, 1859.
(44) Stephenson, H. P.; Sponer, H. *J. Am. Chem. Soc.* **1957**, *79*, 2050.
(45) Liu, W. T.; Thorp, H. H. *Inorg. Chem.* **1993**, *32*, 4102.
(46) Coxall, R. A.; Harris, S. G.; Henderson, D. K.; Parsons, S.; Tasker, P. A.; Winpenny, R. E. P. *Dalton Trans.* **2000**, 2349.
(47) Baikie, A. R. E.; Hursthouse, M. B.; New, L.; Thornton, P.; White, R. G. *J. Am. Chem. Soc. Commun.* **1980**, 684.
(48) Baikie, A. R. E.; Hursthouse, M. B.; New, D. B.; Thornton, P. *J. Am. Chem. Soc. Commun.* **1978**, 62.
(49) Wang, S.; Wemple, M. S.; Yoo, J.; Folting, K.; Huffman, J. C.; Hagen, K. S.; Hendrckson, D. N.; Christou, G. *Inorg. Chem.* **2000**, *39*, 1501.
(50) Cañada-Vilalta, C.; Huffman, J. C.; Christou, G. *Polyhedron.* **2001**, *20*, 1785.

Table 2. Selected Bond Lengths (Å) and Bond Angles (deg) for Complex **1**

Mn(1)−O(3)	1.807(4)	Mn(2)−N(4)	2.206(6)	Mn(4)−O(13)	2.175(4)
Mn(1)−O(7)	1.991(4)	Mn(3)−O(3)	1.867(4)	Mn(4)−O(9)	2.250(4)
Mn(1)−O(4)	2.007(4)	Mn(3)−O(1)	1.899(3)	Mn(5)−O(6)	1.878(4)
Mn(1)−N(1)	2.101(5)	Mn(3)−O(15)	1.938(4)	Mn(5)−O(1)	1.885(4)
Mn(1)−O(14)	2.120(4)	Mn(3)−O(19)	1.997(4)	Mn(5)−O(2)	1.970(4)
Mn(1)−N(2)	2.190(6)	Mn(3)−O(9)	2.229(4)	Mn(5)−O(17)	2.001(5)
Mn(2)−O(2)	1.831(4)	Mn(3)−O(16)	2.246(4)	Mn(5)−O(12)	2.203(4)
Mn(2)−O(8)	1.975(4)	Mn(4)−O(1)	1.871(4)	Mn(5)−O(3)	2.208(4)
Mn(2)−O(5)	2.006(5)	Mn(4)−O(2)	1.904(4)	Mn(3)···Mn(5)	2.9892(12)
Mn(2)−N(3)	2.091(5)	Mn(4)−O(11)	1.912(5)	Mn(3)···Mn(4)	2.9928(12)
Mn(2)−O(10)	2.133(5)	Mn(4)−O(20)	1.971(4)	Mn(4)···Mn(5)	2.8442(13)
O(3)−Mn(1)−O(7)	95.83(17)	O(2)−Mn(2)−N(4)	97.93(18)	O(11)−Mn(4)−O(20)	86.9(2)
O(3)−Mn(1)−O(4)	93.97(16)	O(8)−Mn(2)−N(4)	166.70(19)	O(1)−Mn(4)−O(13)	87.78(17)
O(7)−Mn(1)−O(4)	98.21(18)	O(5)−Mn(2)−N(4)	82.89(19)	O(2)−Mn(4)−O(13)	88.94(16)
O(3)−Mn(1)−N(1)	174.3(2)	N(3)−Mn(2)−N(4)	77.2(2)	O(11)−Mn(4)−O(13)	90.35(19)
O(7)−Mn(1)−N(1)	89.9(2)	O(10)−Mn(2)−N(4)	82.5(2)	O(20)−Mn(4)−O(13)	94.51(17)
O(4)−Mn(1)−N(1)	84.84(17)	O(3)−Mn(3)−O(1)	85.09(16)	O(1)−Mn(4)−O(9)	84.32(15)
O(3)−Mn(1)−O(14)	95.35(17)	O(3)−Mn(3)−O(15)	100.55(18)	O(2)−Mn(4)−O(9)	87.29(15)
O(7)−Mn(1)−O(14)	90.9(2)	O(1)−Mn(3)−O(15)	173.72(17)	O(11)−Mn(4)−O(9)	97.80(18)
O(4)−Mn(1)−O(14)	166.24(18)	O(3)−Mn(3)−O(19)	172.00(17)	O(20)−Mn(4)−O(9)	88.20(16)
N(1)−Mn(1)−O(14)	84.88(17)	O(1)−Mn(3)−O(19)	86.99(17)	O(6)−Mn(5)−O(1)	169.34(16)
O(3)−Mn(1)−N(2)	97.32(18)	O(15)−Mn(3)−O(19)	87.42(18)	O(6)−Mn(5)−O(2)	93.33(17)
O(7)−Mn(1)−N(2)	166.81(16)	O(3)−Mn(3)−O(9)	90.66(16)	O(1)−Mn(5)−O(2)	82.14(16)
O(4)−Mn(1)−N(2)	81.98(18)	O(1)−Mn(3)−O(9)	84.28(14)	O(6)−Mn(5)−O(17)	97.2(2)
N(1)−Mn(1)−N(2)	77.0(2)	O(15)−Mn(3)−O(9)	98.32(17)	O(1)−Mn(5)−O(17)	88.68(18)
O(14)−Mn(1)−N(2)	86.81(19)	O(19)−Mn(3)−O(9)	87.42(17)	O(2)−Mn(5)−O(17)	167.24(18)
O(2)−Mn(2)−O(8)	94.14(16)	O(3)−Mn(3)−O(16)	89.27(16)	O(6)−Mn(5)−O(12)	101.52(17)
O(2)−Mn(2)−O(5)	96.00(17)	O(1)−Mn(3)−O(16)	88.29(15)	O(1)−Mn(5)−O(12)	87.71(16)
O(8)−Mn(2)−O(5)	101.5(2)	O(15)−Mn(3)−O(16)	89.01(18)	O(2)−Mn(5)−O(12)	84.67(17)
O(2)−Mn(2)−N(3)	174.26(19)	O(19)−Mn(3)−O(16)	91.62(17)	O(17)−Mn(5)−O(12)	86.15(19)
O(8)−Mn(2)−N(3)	90.4(2)	O(9)−Mn(3)−O(16)	172.55(15)	O(6)−Mn(5)−O(3)	94.98(15)
O(5)−Mn(2)−N(3)	86.5(2)	O(1)−Mn(4)−O(2)	84.27(16)	O(1)−Mn(5)−O(3)	76.49(14)
O(2)−Mn(2)−O(10)	94.06(19)	O(1)−Mn(4)−O(11)	174.28(18)	O(2)−Mn(5)−O(3)	100.47(15)
O(8)−Mn(2)−O(10)	91.1(2)	O(2)−Mn(4)−O(11)	101.10(18)	O(17)−Mn(5)−O(3)	85.85(18)
O(5)−Mn(2)−O(10)	163.24(18)	O(1)−Mn(4)−O(20)	87.82(17)	O(12)−Mn(5)−O(3)	162.43(15)
N(3)−Mn(2)−O(10)	82.3(2)	O(2)−Mn(4)−O(20)	171.24(18)	Mn(4)−O(1)−Mn(5)	98.45(16)
Mn(4)−O(1)−Mn(3)	105.09(17)	Mn(5)−O(1)−Mn(3)	104.39(18)	Mn(2)−O(2)−Mn(4)	124.3(2)
Mn(2)−O(2)−Mn(5)	137.6(2)	Mn(4)−O(2)−Mn(5)	94.46(15)	Mn(1)−O(3)−Mn(3)	123.8(2)
Mn(1)−O(3)−Mn(5)	133.01(19)	Mn(3)−O(3)−Mn(5)	94.00(16)	Mn(3)−O(9)−Mn(4)	83.84(12)

Scheme 1

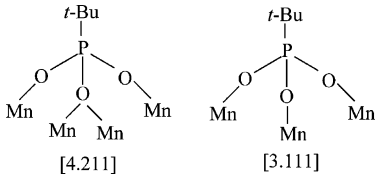

complexes. The four manganese atoms are all in the +3 oxidation state according to the bond valence sum calculations.[45] The two bicapping μ_3-*tert*-butylphosphonate ligands

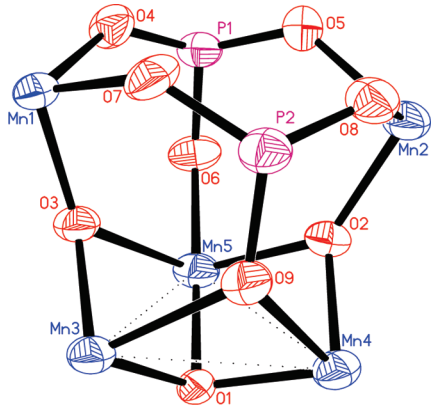

Figure 2. Inorganic core of compounds **1** and **2** showing 30% probability displacement ellipsoids.

in **3**, adopting a [3.111] binding mode by the Harris notation (Scheme 1), are above or below the Mn_4 plane, each binding to three manganese centers of the Mn_3O triangular unit (Figure 4). The distance between the two planes formed by {O(2)−O(3)−O(4)} and {Mn(1)−Mn(2)−Mn(1A)−Mn(2A)} is 2.0466 Å while the distances of P(1)···P(1A) are 5.833 Å. In addition to two capping *tert*-butylphosphonate ligands, there are a total of four bridging μ_2-$MeCO_2^-$ groups around the four Mn atoms and two terminal bpy groups, giving a six-coordination near-octahedral geometry around each Mn^{III} with Jahn−Teller elongation.

As shown in Figures 3b and 4, the molecular structure of complex **4** closely resembles that of **3**, and it possesses an identical inorganic core structure to **3** but the peripheral ligation of $PhCOO^-$ groups in **4** substitutes $MeCO_2^-$ groups in **3**. A comparison of selected bonds distances and angles of **3** with those of **4** is given in Supporting Information, Table S2.

$NBu^n_4[Mn_4O_2(EtCOO)_3(MeCOO)_4(pic)_2]$ (5), $NR'_4[Mn_4O_2(i\text{-}PrCOO)_7(pic)_2]$ ($R' = Bu^n$, (6); $R' =$ Et, (7)). The ORTEP diagram for the anion of complex **5** is shown in Supporting Information, Figure S1, and selected bond lengths and angles for **5** are given in Supporting Information, Table S3. The anion contains a $[Mn_4(\mu_3\text{-}O)_2]^{8+}$ core in which the four Mn atoms display a folded "butterfly-like" conformation just as in some previously reported $[Mn_4(\mu_3\text{-}O)_2]^{8+}$ com-

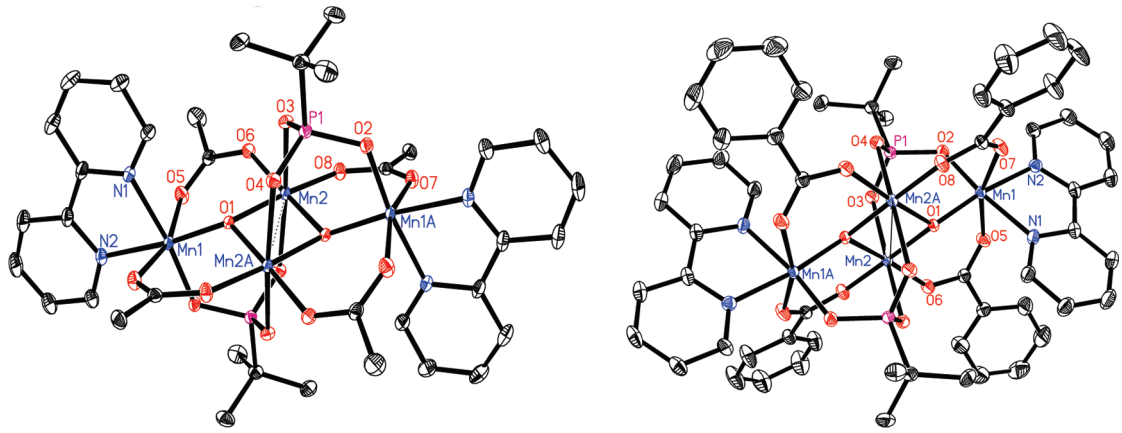

(a) (b)

Figure 3. Crystal structures of (a) compound **3** and (b) compound **4** at 30% probability displacement ellipsoids. Hydrogen atoms have been omitted for clarity.

Table 3. Selected Bond Lengths (Å) and Bond Angles (deg) for Complex **3**

Mn(1)−O(2A)	1.8659(15)	Mn(2)−O(1)	1.9086(15)
Mn(1)−O(1)	1.8693(14)	Mn(2)−O(6)	1.9358(16)
Mn(1)−N(2)	2.0465(19)	Mn(2)−O(8)	1.9401(16)
Mn(1)−N(1)	2.0475(19)	Mn(2)−O(3)	2.1949(16)
Mn(1)−O(7A)	2.2086(17)	Mn(2)−O(4A)	2.3362(16)
Mn(1)−O(5)	2.2136(17)	Mn(2)···Mn(2A)	2.8380(9)
Mn(2)−O(1A)	1.9055(14)		

O(2A)−Mn(1)−O(1)	95.42(7)	O(1A)−Mn(2)−O(1)	83.84(6)
O(2A)−Mn(1)−N(2)	91.39(8)	O(1A)−Mn(2)−O(6)	177.10(6)
O(1)−Mn(1)−N(2)	173.18(7)	O(1)−Mn(2)−O(6)	96.73(6)
O(2A)−Mn(1)−N(1)	170.08(7)	O(1A)−Mn(2)−O(8)	96.34(6)
O(1)−Mn(1)−N(1)	93.99(7)	O(1)−Mn(2)−O(8)	174.39(7)
N(2)−Mn(1)−N(1)	79.21(8)	O(6)−Mn(2)−O(8)	83.38(7)
O(2A)−Mn(1)−O(7A)	98.87(7)	O(1A)−Mn(2)−O(3)	89.54(6)
O(1)−Mn(1)−O(7A)	92.35(7)	O(1)−Mn(2)−O(3)	88.43(6)
N(2)−Mn(1)−O(7A)	86.42(7)	O(6)−Mn(2)−O(3)	87.63(7)
N(1)−Mn(1)−O(7A	83.85(7)	O(8)−Mn(2)−O(3)	97.18(7)
O(2A)−Mn(1)−O(5)	94.01(7)	O(1A)−Mn(2)−O(4A)	86.62(6)
O(1)−Mn(1)−O(5)	95.58(7)	O(1)−Mn(2)−O(4A)	84.18(6)
N(2)−Mn(1)−O(5)	84.08(7)	O(6)−Mn(2)−O(4A)	96.27(7)
N(1)−Mn(1)−O(5)	81.95(8)	O(8)−Mn(2)−O(4A)	90.23(6)
O(7A)−Mn(1)−O(5)	164.17(6)	O(3)−Mn(2)−O(4A)	172.00(5)

plexes.[4d,51–53] The whole structure of **5** is very similar to that of $NBu^n_4[Mn_4O_2(RCOO)_7(pic)_2]$ (R = Me, Et, Ph).[4d] It is worthwhile to point out that there are two kinds of carboxylate groups (three $EtCOO^-$ and four $MeCOO^-$) in complex **5** that have not been obtained before. Three $EtCOO^-$ groups in **5** replace three of the seven $MeCOO^-$ groups in $NBu^n_4[Mn_4O_2(MeCOO)_7(pic)_2]$.[4d]

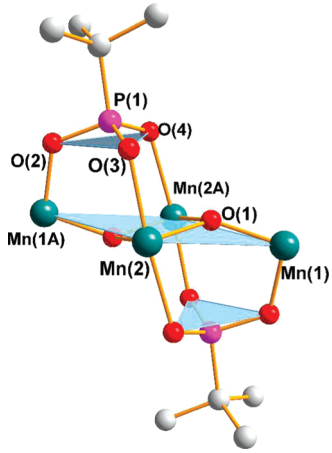

Figure 4. DIAMOND view of the core of **3** and **4** showing the planar parallelogram Mn_4 array bicapped by the $[t\text{-}BuPO_3]^{2-}$.

As shown in Supporting Information, Figure S1, the anions of complexes **6** and **7** possess similar structures to that of **5**. A comparison of selected bond distances and angles of **5** with those of **6** and **7** is given in Supporting Information, Table S4.

Magnetic Susceptibility Studies. Magnetic susceptibility data for **1·2H₂O·MeOH·MeCN**, **3·6H₂O·2MeCOOH**, and **5·0.5H₂O** were measured in the temperature range 2−300 K under a field of 0.5 T. The resulting plots of χ_M and $\chi_M T$ versus T for **1**, **3**, and **5** are depicted in Figures 5, top, and 7, top, and in Supporting Information, Figure S2, respectively.

As the temperature is lowered, the $\chi_M T$ of complex **1** decreases smoothly from a value of 11.04 $cm^3\ mol^{-1}\ K$ at 300 K to 5.50 $cm^3\ mol^{-1}\ K$ at 16 K, and then the value falls sharply to 3.15 $cm^3\ mol^{-1}\ K$ at 2 K. The $\chi_M T$ value (11.05 $cm^3\ mol^{-1}\ K$) at room temperature is smaller than that of 14.99 $cm^3\ mol^{-1}\ K$ expected for five independent Mn(III) ions with $S = 2$. This result reveals the overall intramolecular antiferromagnetic character of the system. As shown in Figure 5, bottom, a model is used to simulate the exchange interaction within the complex, which involves five pairwise couplings on the basis of the bridge angles and the distances between the Mn atoms. The susceptibility data were fitted using the magnetism package MAGPACK[54,55] based on the interaction pattern (Figure 5, bottom) and on the corresponding Hamiltonian (eq 1).

(51) Wang, B. S.; Huffman, J. C.; Folting, K.; Streib, W. E.; Lobkovsky, E. B.; Christou, G. *Angew. Chem., Int. Ed. Engl.* **1991**, *30*, 1672.
(52) Wemple, M. W.; Tsai, H. L.; Wang, S.; Claude, J. P.; Streib, W. E.; Huffman, J. C.; Hendrickson, D. N.; Christou, G. *Inorg. Chem.* **1996**, *35*, 6437.
(53) Huang, D.; Zhang, X.; Ma, C.; Chen, H.; Chen, C.; Liu, Q.; Zhang, C.; Liao, D.; Li, L. *Dalton Trans.* **2007**, 680.
(54) Borrás-Almenar, J. J.; Clemente-Juan, J. M.; Coronado, E.; Tsukerblat, B. S. *J. Comput. Chem.* **2001**, *22*, 985.
(55) Borrás-Almenar, J. J.; Clemente-Juan, J. M.; Coronado, E.; Tsukerblat, B. S. *Inorg. Chem.* **1999**, *38*, 6081.

$$\hat{H} = -2J_1\hat{S}_3\hat{S}_4 - 2J_2(\hat{S}_3\hat{S}_5 + \hat{S}_4\hat{S}_5) - 2J_3(\hat{S}_1\hat{S}_3 + \hat{S}_2\hat{S}_4) - 2J_4(\hat{S}_1\hat{S}_5 + \hat{S}_2\hat{S}_5) - 2J_5\hat{S}_1\hat{S}_2 \quad (1)$$

Several sets of fitted parameters have been obtained by choosing different starting values of J, two of which with acceptable convergence values (R) are (i) $J_1 = -5.59\ cm^{-1}$, $J_2 = 15.40\ cm^{-1}$, $J_3 = 16.15\ cm^{-1}$, $J_4 = -46.53\ cm^{-1}$, $J_5 = 2.73\ cm^{-1}$, $g = 2.01$, $R = 6.87 \times 10^{-5}$, and (ii) $J_1 = -2.18\ cm^{-1}$, $J_2 = 6.93\ cm^{-1}$, $J_3 = -13.94\ cm^{-1}$, $J_4 = -9.62\ cm^{-1}$, $J_5 = -11.17\ cm^{-1}$, $g = 2.00$ and $R = 6.27 \times 10^{-4}$ (Defined as $\sum[(\chi_M T)_{calcd.} - (\chi_M T)_{obsd.}]^2/[\sum(\chi_M T)_{obsd.}]^2$). Obviously, the coupling interactions between the paramagnetic metal ions are sensitive to the type of bridge between the metal centers, as well as the related structure parameters. There is no literature about magnetostructural correlations between the structure parameters (such as $Mn^{III}-O-Mn^{III}$ angle) and the sign/magnitude of the exchange constant for such a complicated system; however, we can tentatively discuss the correlations by comparison with some reported dinuclear manganese clusters with a $[Mn^{III}_2O]$ core.[56] In these dinuclear manganese clusters, the angles of the $Mn^{III}-O-Mn^{III}$ bridges transmitting the exchange interactions of -6.8, $+9$, -0.5, and $-120\ cm^{-1}$ are 122.9°, 118°, 125°, and 168°, respectively, which exhibit some similarities in the $Mn^{III}-O-Mn^{III}$ angles with those (~105°, ~94°, ~124°, ~135°, respectively, found in our compounds) corresponding to the first four

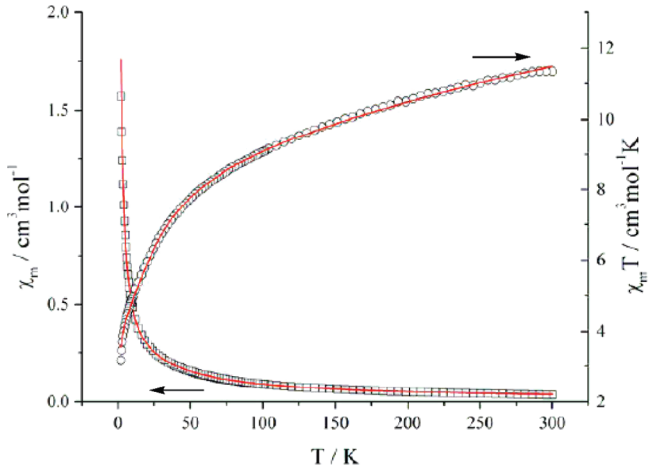

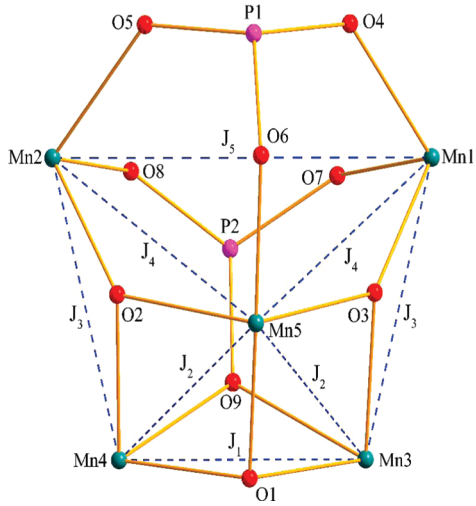

Figure 5. (top) Temperature dependence of χ_m (□) and $\chi_m T$ (○) values for **1**·2H$_2$O·MeOH·MeCN. The solid lines correspond to the best-fit curves using the parameters described in the text. (bottom) Spin topology for **1**·2H$_2$O·MeOH·MeCN assuming five different J values.

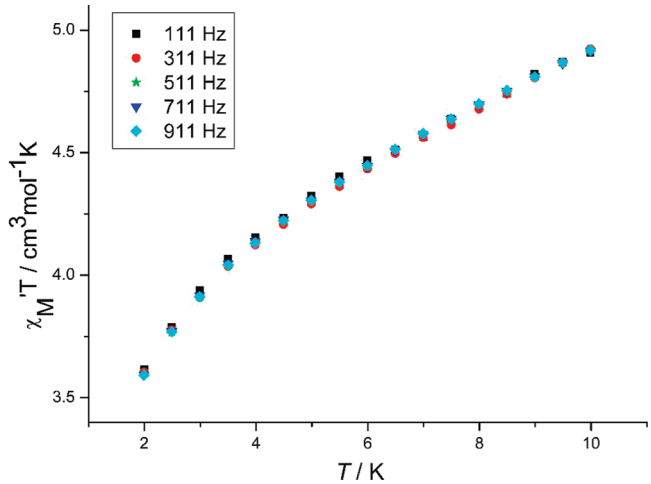

Figure 6. Plots of in-phase ($\chi_M'T$) ac susceptibility versus temperature (T) for **1**·2H$_2$O·MeOH·MeCN.

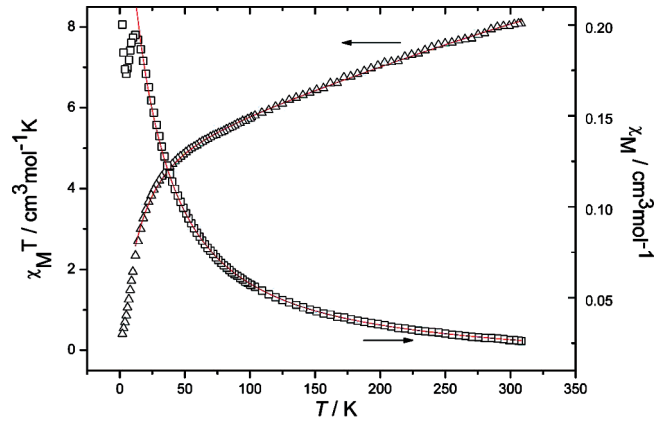

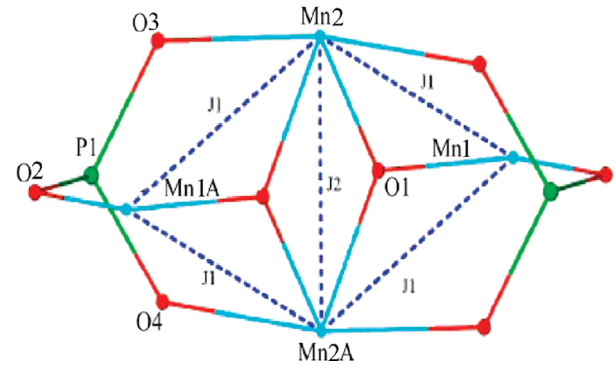

Figure 7. (top) Temperature dependence $\chi_M T$ (△) and χ_M (□) values for **3**·6H$_2$O·2MeCOOH. The solid lines correspond to the best-fit curves using the parameters described in the text. (bottom) Spin topology for **3**·6H$_2$O·2MeCOOH assuming two different J values.

(56) (a) Hotzelmann, R.; Wieghardt, K.; Flörke, U.; Haupt, H.-J.; Weatherburn, D. C.; Bonvoisin, J.; Blondin, G.; Girerd, J.-J. *J. Am. Chem. Soc.* **1992**, *114*, 1681. (b) Kipke, C. A.; Scott, M. J.; Gohdes, J. W.; Armstrong, W. H. *Inorg. Chem.* **1990**, *29*, 2193. (c) Wieghardt, K.; Bossek, U.; Nuber, B.; Weiss, J.; Bonvoisin, J.; Corbella, M.; Vitols, S. E.; Girerd, J. J. *J. Am. Chem. Soc.* **1988**, *110*, 7398. (d) Wieghardt, K.; Bossek, U.; Ventur, D.; Weiss, J. *J. Chem. Soc. Commun.* **1985**, 347. (e) Ménage, S.; Girerd, J. J.; Gleizes, A. *J. Chem. Soc. Commun.* **1988**, 431.

interactions (J_1-J_4). Besides these $Mn^{III}-O-Mn^{III}$ bridges, the other external bridges in our complex (O−P−O and O−C−O bridges) exhibit partial similarity to these reported dinuclear manganese clusters (O−C−O bridges). So we think that the second set of the fitted parameters is a more reasonable result. As for J_5, there is no $Mn^{III}-O-Mn^{III}$ bridge between Mn1 and Mn2 but two O−P−O bridges which usually can mediate the antiferromagnetic exchange.[57]

As shown in Supporting Information, Figure S3, the isothermal magnetization values $M(H)$ of complex **1** were collected at 2 K but no hysteresis loop was observed. The alternating current (ac) magnetic susceptibility measurement was carried out with a 3.0 G ac field at frequencies of 111, 311, 511, 711, and 911 Hz without the use of a dc field. As seen from Figure 6, the in-phase signal ($\chi_M'T$) is not frequency-dependent, and the extrapolation of the plot to the lowest temperature 0 K affords a $\chi_M'T$ value of about 3 cm^3 mol^{-1} K, indicating an $S = 2$ ground-state with $g = 2.00$. All the results suggest that complex **1** is not a single molecular magnet (SMM).

The χ_MT value at 300 K is 8.08 cm^3 mol^{-1} K for compound **3**; upon cooling, the value of χ_MT gradually decreases to 4.20 cm^3 mol^{-1} K at 30 K, whereupon the value falls sharply to 0.40 cm^3 mol^{-1} K at 2 K. The χ_MT per Mn4 at room temperature (8.08 and 8.04 cm^3 mol^{-1} K for **3** and **5**, respectively) is smaller than that of 12.01 cm^3 mol^{-1} K expected for four independent Mn(III) ions with $S = 2$, which indicates the overall antiferromagnetic character of the two systems. As shown in Figure 7, bottom, a model is used to simulate the antiferromagnetic exchange interaction within complex **3** which involves two pairwise couplings, J_1 corresponding to the interactions between Mn(1) and Mn(2) joined by one μ_3-O, one O−P−O and one O−C−O bridge, J_2 corresponding to the interactions between Mn(2) and Mn(2A) connected by two μ_3-O and two O−P−O bridges. The susceptibility data of **3** and **5** were fitted over the temperature range 20−300 K based on the interaction patterns shown in Figure 7, bottom, and Supporting Information, Figure S2, bottom, respectively, and on the corresponding Hamiltonian (eq 2).

$$\hat{H} = -2J_1(\hat{S}_1\hat{S}_2 + \hat{S}_1\hat{S}_3 + \hat{S}_2\hat{S}_4 + \hat{S}_3\hat{S}_4) - 2J_2\hat{S}_1\hat{S}_4 \qquad (2)$$

The molecular field approximation (zJ')[58] is introduced to estimate the inter-complex interactions, and the best-fit parameters obtained are $J_1 = -5.41$ cm^{-1}, $J_2 = -35.44$ cm^{-1}, $g = 2.13$, $zJ' = -1.55$ cm^{-1}, and $R = 2.15 \times 10^{-4}$ for **3**, and $J_1 = -2.29$ cm^{-1}, $J_2 = -35.21$ cm^{-1}, $g = 2.02$, $zJ' = -0.86$ cm^{-1}, and $R = 3.15 \times 10^{-4}$ for **5** (R is defined as $\sum[(\chi_MT)_{calcd.} - (\chi_MT)_{obsd.}]^2/[\sum(\chi_MT)_{obsd.}]^2$). The results reveal the overall antiferromagnetic character of the systems of **3** and **5**, which are comparable to those of known tetranuclear Mn(III) complexes,[4d,49] though there are obvious distinctions in structural features between the two types of Mn_4O_2 complexes, including 4Mn coplanarity and phosphonate coordination. This seems to indicate that the phosphonate coordination did not have an essential influence on the magnetic exchange between the Mn(III) ions, indicating also that the μ_3-O bridge may be the strongest mediator for transmitting the exchange interaction between the Mn(III) ions.

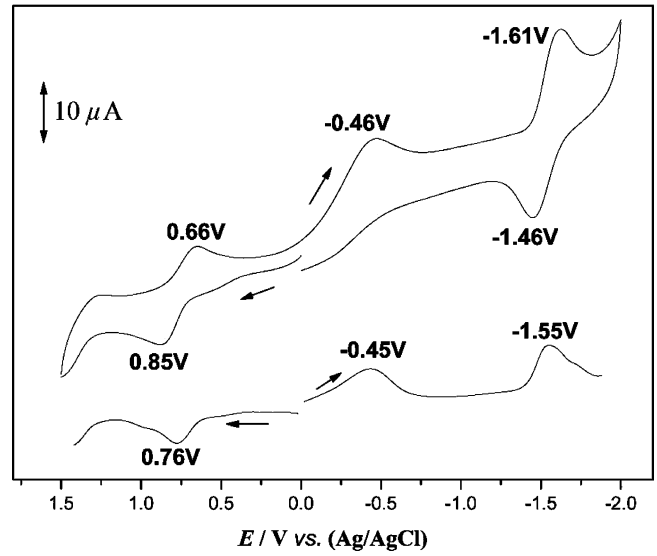

Figure 8. Cyclic voltammogram (100 mV s^{-1}) (top) and differential pulse voltammetry (100 mV s^{-1}) (bottom) for complex **1** in distilled CH_2Cl_2 with 0.1 M $NBu^n_4PF_6$ as supporting electrolyte.

Electrochemical Studies. The cyclic voltammetry (CV) and differential pulse voltammetry (DPV) of **1**, **3**, and **5** have been recorded in distilled CH_2Cl_2 solution under argon in the presence of 0.1 M $NBu^n_4PF_6$ as supporting electrolyte.

As the CV and DPV plots (Figure 8) show, compound **1** displays two quasi-reversible waves at $E_{1/2} = 0.76$ V ($\Delta E_P = 190$ mV) and $E_{1/2} = \sim -1.54$ V ($\Delta E_P = 150$ mV) versus Ag/AgCl and one irreversible reduction at ~ -0.46 V between both the quasi-reversible redox waves. (Under the same experimental condition, the Fc/Fc^+ couple is at $E_{1/2} = 0.436$ V.) The first two quasi-reversible redox waves with the relatively small peak separations are comparable to that of the Fc/Fc^+ couple under the same condition, suggesting that they are all one-electron processes.[59] Also, the studies of the changes in the redox processes at the scan rate of 100, 200, 300, 500, and 800 mV s^{-1} indicate that the processes at 0.46 and −1.54 V are quasi-reversible (Supporting Information, Figure S4). The deprotonated ligand t-$BuPO_3^{2-}$ does not display any such peaks as mentioned above. Thus, the redox processes are all metal-based, which are consistent with the electrochemistry of the other reported manganese clusters.[4a,d,m] The quasi-reversible oxidation at the $E_{1/2}$ value of 0.76 V is tentatively assigned to the oxidation of Mn^{III}_5 to $Mn^{III}_4Mn^{IV}$. An *in situ* UV−vis−NIR

(57) (a) Ikotou, O. F.; Armatus, N. G.; Julve, M.; Kruger, P. E.; Lloret, F.; Nieuwenhuyzen, M.; Doyle, R. P. *Inorg. Chem.* **2007**, *46*, 6668. (b) Sanz, F.; Parada, C.; Rojo, J. M.; Ruíz-Valero, C. *Chem. Mater.* **2001**, *13*, 1334. (c) Bu, X.; Feng, P.; Stucky, G. D. *J. Solid State Chem.* **1997**, *131*, 387. (d) Fan, J.; Yee, G. T.; Wang, G.; Hanson, B. E. *Inorg. Chem.* **2006**, *45*, 599.

(58) χ_0 is the susceptibility of the noninteracting compounds, z is the number of nearest neignbors, and J' is the magnetic interactions between units. See Kachi-Terajima, C.; Miyasaka, H.; Sugiura, K.-i.; Clérac, R.; Nojin, H. *Inorg. Chem.* **2006**, *45*, 4381.

(59) Sessoli, R.; Tsai, H.-L.; Schake, A. R.; Wang, S.; Vincent, J. B.; Folting, K.; Gatteschi, D.; Christou, G;.; Hendrickson, D. N. *J. Am. Chem. Soc.* **1993**, *115*, 1804.

spectroelectrochemistry of compound **1** was tested from 0.6 to 1.0 V. Two absorption bands occurred at 235 and 270 nm, and no obvious absorption was observed in the range >400 nm. Meanwhile, no spectral change was observed in the testing process. This seems a hint that both the ligands and the skeleton of the complex may remain intact in the oxidation. It is noticed that polynuclear Mn(III) clusters may be insensitive in the visible range to the variation of the Mn oxidation states because the solutions of these Mn(III) clusters are usually dark or black. So far UV−vis data for the polynuclear Mn phosphate clusters still remain absent, while related UV−vis data[60] or studies[61] are rarely reported for other polynuclear Mn clusters. Subsequent irreversible reduction at −0.46 V implies the occurrence of some chemical reactions that follow some electrochemical processes. A new optical band at 245 nm was observed with *in situ* UV−vis−NIR spectroelectrochemistry from −0.2 to −0.8 V, acompanying the weakening of the original bands at 233 and 272 nm, which can commonly be attributed to the variation of metal−ligand linkage (ligand loss or structural rearrangement, etc.) in the chemical reaction. Also the ligands (*t*-$BuPO_3H_2$ + phen) showed two bands at 227 and 263 nm in the same testing conditions to that for **1**, implying that the new band seems not to be from the free ligands. However, it is difficult to analyze what variation occurs in this irreversible reduction. Interestingly, the second reduction at −1.54 V is a quasi-reversible one-electron process. We attempted to isolate the possible species in the solution but failed.

The CV and DPV plots of compound **5** (Supporting Information, Figures S5 and S6) show that there is an irreversible reduction response at ∼ −0.46 V versus Ag/AgCl which is comparable to that of the similar tetranuclear Mn(III) complexes.[4d] In addition, an irreversible oxidation at about 0.57 V and one quasi-reversible wave at $E_{1/2} = 1.00$ V ($\Delta E_P = 160$ mV) were observed. Consulting the electrochemical behaviors[4d] of similar tetranuclear Mn(III) complexes, the latter redox can be assigned to the $Mn^{III}{}_4$/$Mn^{III}{}_3Mn^{IV}$ couple. The difference of the values of last two peaks is considered to stem from the various carboxylate ligands.[62]

The oxidative and reductive electrochemistry of compound **3** was studied using CV and DPV in the potential range from 1.5 to −1 V versus Ag/AgCl (Figure 9). Compound **3** has a similar electrochemical behavior as that of compound **5** and other Mn_4O_2 clusters.[4d,m,63] It displays one irreversible reduction response at ∼ −0.50 V when scanning toward the cathodic potential and one quasi-reversible wave at $E_{1/2}$ = ∼ 0.74 V ($\Delta E_P = 230$ mV) when scanning toward the anodic

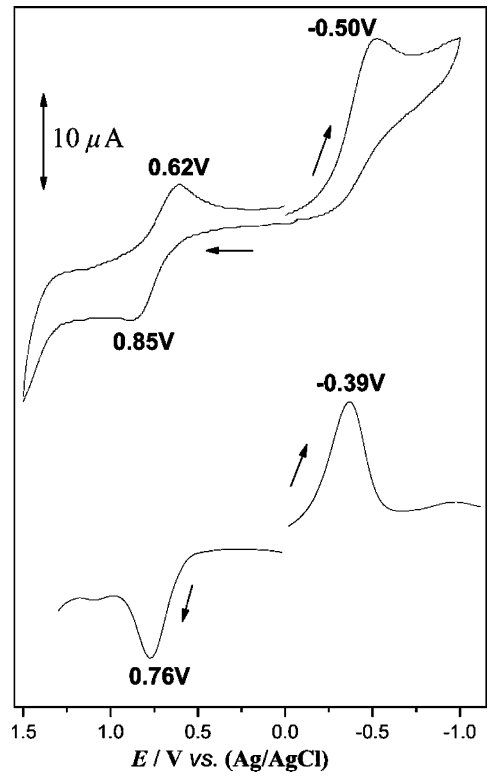

Figure 9. Cyclic voltammogram (100 mV s^{-1}) (top) and differential pulse voltammetry (100 mV s^{-1}) (bottom) for complex **3** in distilled CH_2Cl_2 with 0.1 M $NBu^n{}_4PF_6$ as supporting electrolyte.

potential. Consulting the assignment for complex **5**, the quasi-reversible redox can be assigned to the $Mn^{III}{}_4$/$Mn^{III}{}_3Mn^{IV}$ couple. The studies of the changes in the reduction and oxidation processes at the sweeping potential range from 0 to 1.5 V and at the scan rate of 100, 200, 300, 500, and 800 mV s^{-1} also indicate that the $Mn^{III}{}_4$/$Mn^{III}{}_3Mn^{IV}$ couple is quasi-reversible (Supporting Information, Figure S7). The *in situ* UV−vis−NIR spectroelectrochemistry of compound **3** was studied, and there was no obvious change of the spectra in the reduction (−0.2 ∼ −0.7 V) and oxidation processes (0.4 ∼ 1.0 V). The unvaried peak at 291 nm implies the stability of the metal−ligand linkage in the complex. Complex **3** did not exhibit an obvious signal in the range of 400−900 nm in the whole redox process, owing to the insensitivity of the polynuclear Mn(III) cluster in visible range though one of the Mn(III) ions was oxidized.

The ESI-MS of the CH_2Cl_2 solution of **1**, **3**, and **5** gave major peaks at *m*/*z* 1269.7, 1096.7, and 1192.5, which correspond to $[\mathbf{1} + H]^+$, $[\mathbf{3} + Na]^+$, and $[\mathbf{5} + H]^+$ (positive mode), suggesting the stability of the complexes in solution, which also gives support for the assignment of the electrochemistry processes of the three complexes.

Conclusions

In summary, the *t*-$BuPO_3H_2$−Mn^{2+}−RCOOH reaction system has been systematically explored, and it is observed that the use of different N-containing coligands (bpy, phen, and pic) in this reaction system leads to three completely different types of manganese clusters (**1**−**7**), that is, pentanuclear clusters with phosphonate ligands, tetranuclear

(60) (a) Wemple, M. W.; Tsai, H.-L.; Wang, S.; Claude, J. P.; Streib, W. E.; Huffman, J. C.; Hendrickson, D. N.; Christou, G. *Inorg. Chem.* **1996**, *35*, 6437. (b) Vincent, J. B.; Christmas, C.; Chang, H. R.; Li, Q.; Boyd, P. D. W.; Huffman, J. C.; Hendrickson, D. N.; Christou, G. *J. Am. Chem. Soc.* **1989**, *111*, 2086.
(61) Carrell, T. G.; Bourles, E.; Lin, M.; Dismukes, G. C. *Inorg. Chem.* **2003**, *42*, 2849.
(62) Chakov, N. E.; Zakharov, L. N.; Rheingold, A. L.; Abboud, K. A.; Christou, G. *Inorg. Chem.* **2005**, *44*, 4555.
(63) (a) Boskovic, C.; Folting, K.; Christou, G. *Polyhedron* **2000**, *19*, 2111. (b) Aromí, G.; Bhaduri, S.; Artús, P.; Huffman, J. C.; Hendrickson, D. N.; Christou, G. *Polyhedron* **2002**, *21*, 1779.

clusters with phosphonate ligands, and tetranuclear clusters without phosphonate ligands, which demonstrates the control of these N-containing coligands over the framework of the manganese clusters. The pentanuclear cluster with a basket-like core is a novel structural type among the manganese phosphonates. The experimental finding provides an important addition to the study of manganese phosphonate chemistry. The magnetic property of the pentanuclear cluster **1·2H$_2$O·MeOH·MeCN** shows both ferromagnetic and antiferromagnetic couplings among the Mn atoms, though the overall character is antiferromagnetic. It is also a good example of the influence of O−P−O, μ_3-O, and O−C−O bridges on the magnetic interaction. The results of the magnetic measurements for the other two tetranuclear species reveal antiferromagnetic character as expected for their $[Mn_4(\mu_3\text{-}O)_2]^{8+}$ structure. The effect of N-containing coligands in the reaction system of phosphonic acid on the topology of the manganese clusters and other transition metal clusters will be further exploited in our future work.

Acknowledgment. This work was supported by the National Natural Science Foundation of China (No. 20471061 and No. 20633020) and the Science & Technology Innovation Foundation for the Young Scholar of Fujian Province (No. 2005J059).

Supporting Information Available: X-ray crystallographic files in CIF format for the seven complexes (CIF), three tables, and five figures (PDF). This material is available free of charge via the Internet at http://pubs.acs.org.

IC701343S